XMaS
NEWSLETTER

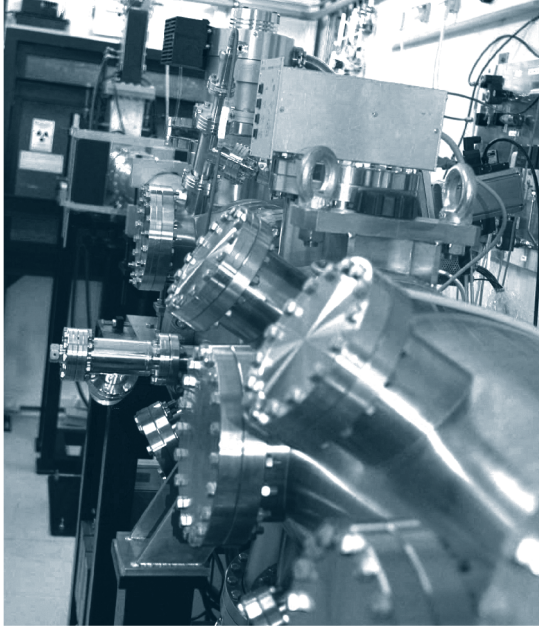

2010

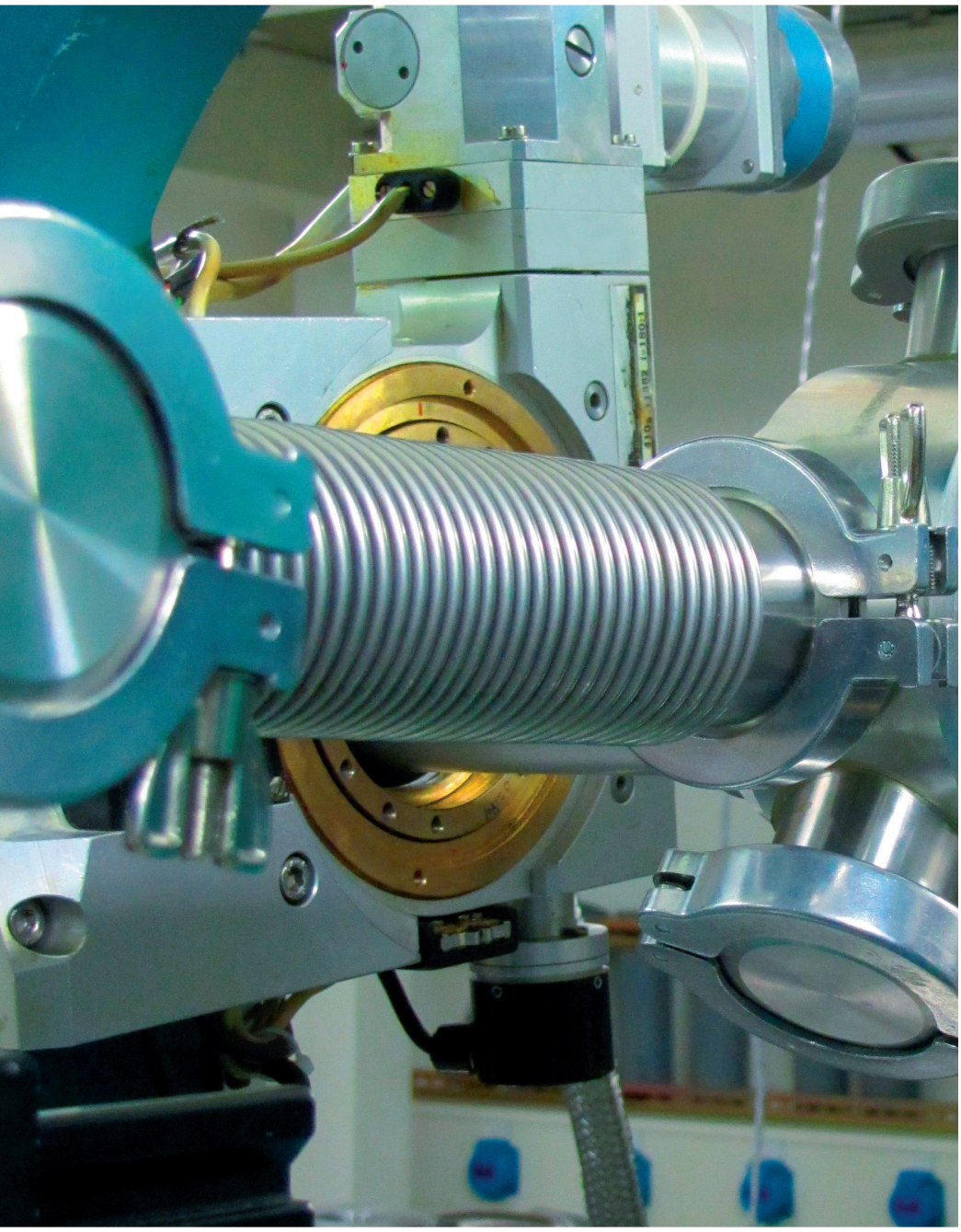

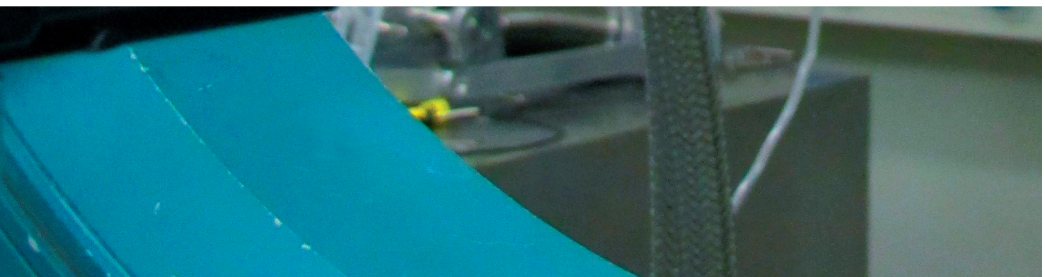

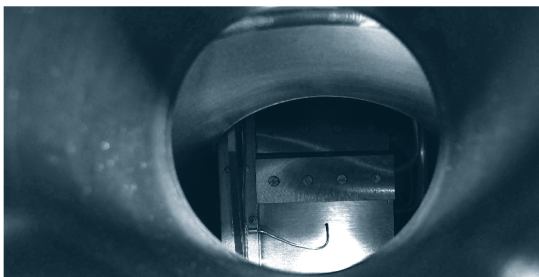

Status

CONTENTS

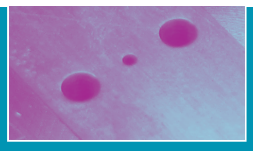

It is a great pleasure to present another XMaS newsletter filled with just a selection of the interesting and exciting science recently performed by our broad community of users, together with news about the development of the beamline.

This year saw a number of changes in personnel on the beamline. Gemma Newby, who has just completed her PhD at Reading accepted the postdoctoral position joint with the UK Diamond Light Source and joined us in April 2010. Oier Bikondoa, who had been originally recruited into that joint role moved over to become a full time member of the beamline team. Peter Normile left to take up a permanent position in his previous group at the University of Castilla-La Mancha, Spain in the autumn. We wish him all the best for a successful future and thank him for his terrific contribution to the XMaS project over the last 3 years. Very recently Didier Wermeille joined us as a beamline scientist. He has most recently worked on the ESRF Surface Diffraction beamline ID03, but prior to that he was at APS and even earlier on ESRF's Magnetic Scattering beamline, ID20 in the "early days". Finally, following Malcolm Cooper's formal retirement from Warwick University, Tom Hase was co-opted as Warwick's Project Director, with Malcolm continuing to work for the XMaS cause.

At the time of writing the beamline is close to changing over to cryo-cooling of the monochromator. The nitrogen line was installed almost one year ago and during the summer of 2010 the monochromator goniometer was re-engineered for liquid nitrogen cooling (but consistent with returning to water cooling if necessary). Now the final piece of the jigsaw – the new cryo-cooled crystal cage – is being installed. We hope that all this effort and expense results in XMaS users having the benefit of a more brilliant and stable beam on their sample. This is not the only beamline development: the energy range has been extended down to 2.035 keV, largely by the replacement of the Be front end with one having a thinner window and a re-design of the crystal assembly to allow a wider range of monochromator Bragg angles. These modifications present exciting new opportunities for scattering studies of 4d and 5d magnetism and - pastures new – the potential to study sulphur and phosphorus K edges in biological materials.

As well as becoming softer, XMaS is offering a new facility allowing electric polarisation measurements with and without x-rays. This facility has been successfully used several times in the last year for the study of multiferroic and ferroelectric materials.
Two examples of work, namely "In-situ electric polarisation measurements of multiferroic $TmMn_2O_5$" and "In-situ real time structural response of ferroelectrics to an external electric field", are presented later in this Newsletter. Currently XMaS offers an electric field sample environment with potentials of ± 2 kV with temperatures down to 2 K in a 4 T magnetic field. A separate sample environment provides ± 10 kV down to 10 K in a 1 T field.

In the autumn of 2010 the UK government published its comprehensive spending review. Although science funding did not suffer the cuts experienced elsewhere, the situation is clearly difficult. We wait, with baited breath, to discover how EPSRC's mid-range facilities, such as XMaS, will be funded. XMaS needs renewal in autumn 2012. Given STFC's recently announced reduction of UK funding for ESRF, the strategic importance of having a UK access point to the world's leading synchrotron facility is paramount.

Finally, the next XMaS User Meeting will take place at Warwick on Friday the 20th of May. Write it down in your diary!

Malcolm Cooper, Tom Hase and Chris Lucas

UNIVERSITY OF LIVERPOOL THE UNIVERSITY OF WARWICK

XMaS going softer!

Over the last few years XMaS has greatly improved the capability at low energies by modifying the beamline, e.g. with thinner Be windows. Initially this enabled studies at the uranium M_5 edge (3.55 keV) but in recent years has included a windowless sample environment that has enabled high quality resonant magnetic scattering at the ruthenium L_2 edge (2.97 keV). The current lowest accessible energy at XMaS is 2.40 keV, which allows studies down to, and including, the sulphur K edge. The design of the new liquid-nitrogen cooled monochromator has been influenced by the need to obtain very low energy x-rays and hence allow resonant studies at previously unobtainable elemental edges.

The new monochromator will allow access to energies down to 2.035 keV. Obviously the flux from the bending magnet is dropping as we push further down in energy, but equally, resonant enhancements are often larger at softer energy edges. The new monochromator design (see **Figure 1**) will enable studies at the phosphorus K edge, which like the sulphur K edge is potentially of great interest to life scientists as phosphorus is an element often present in biological materials. Thus, the new monochromator will enable anomalous scattering experiments and phasing at the phosphorus edge. Other absorption edges that will now become available include the L_3 edges of niobium, zirconium and yttrium as well as the M_5 edges of mercury, gold, platinum and iridium. There are a number of important systems that display charge and magnetic ordering containing these elements that can now be studied using resonant x-ray scattering techniques.

The potential for undertaking experiments at the iridium M_5 edge is potentially of great interest as there are many magnetically ordered iridium mixed metal oxides. Spin glass behaviour has also been seen in iridium pyrochlores and superconductivity in the rare-earth iridium borides. In general magnetism in compounds containing the 4d and 5d elements has been far less studied than those of the 3d elements and the lanthanides. There are very few beamlines anywhere in the world that have the enhanced capability of XMaS for reaching these low energy absorption edges and undertaking resonant x-ray magnetic scattering. The project management committee welcomes proposals from new and existing users to exploit this new x-ray energy range. All of the component parts of the new monochromator have now arrived on the beamline in preparation for its installation.

P.D. Hatton and A.T. Boothroyd on behalf of the Project Management Committee

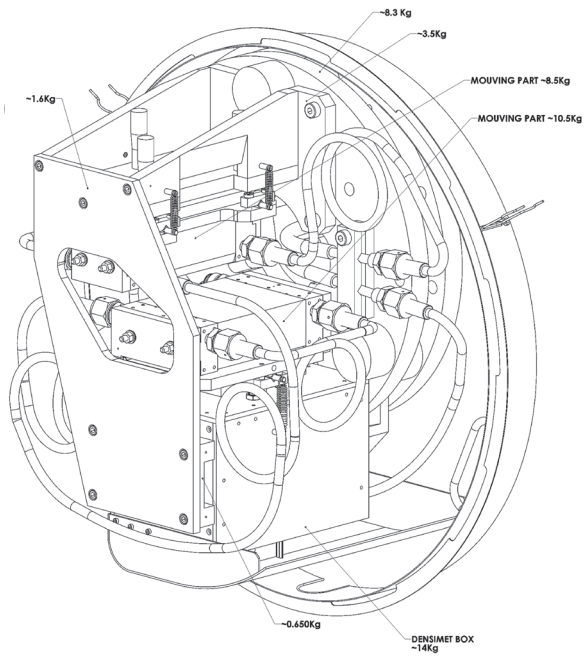

Figure 1: *New monochromator design.*

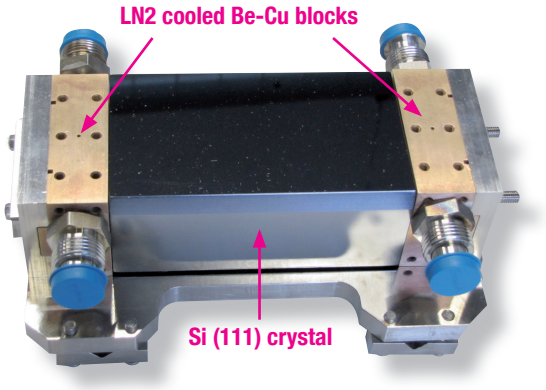

Figure 2: *New monochromator first crystal and crystal mount.*

Probing charge transfer at the electrochemical interface

C.A. Lucas, Y. Gründer and P. Thompson – for further information contact C.A. Lucas, Department of Physics, University of Liverpool, Liverpool, L69 7ZE, UK.

clucas@liverpool.ac.uk

An unsolved and crucial question in electrochemistry is the issue of charge transfer between the metal electrode and the adsorbate as this defines the nature of the bonding. There have been few experimental electrochemical studies due to the complexity of the electrochemical environment which makes the surface inaccessible to most probes of charge transfer. Surface x-ray resonant diffraction (SXRRD) is one of the few techniques that may be applicable for probing the charge distribution at the electrochemical interface. On Cu(100), Br and Cl form ordered c(2x2) adlayers that have been observed in both ultra-high vacuum (UHV) **[1]** and electrochemical studies **[2-3]** (a schematic of the structure is shown in **Figure 3**).

SXRRD analysis of Cu(001)-c(2x2)-Cl (formed in a defined potential range in HCl) showed a corrugation in the second atomic copper layer which is opposite in phase to the corrugation observed for Cu(100)-Cl under UHV conditions. This reveals the importance of charge screening by the solvent molecules and the major influence of the electrochemical double layer on the charge distribution at the interface. The c(2x2) adlayer is a simple structure (the adlayer forms a square structure with a coverage of 0.5 halide atoms per surface Cu atom) and this makes the system an ideal candidate to investigate the suitability of resonant surface x-ray scattering experiments to probe the charge transfer and nature of the chemical bonding *in-situ*.

Measurements through the Cu K edge at the anti-Bragg position of a Cu crystal truncation rod (CTR) for both Br and Cl are shown in **Figure 4**. In both cases the edge shifts to higher energy values compared to the Cu bulk value indicating stronger bound core electrons. In a simple qualitative interpretation this implies that the surface Cu atoms are positively charged. Interestingly, measurements through the Cu K edge at the superstructure rod showed no near-edge shifts indicating that the atoms in the second Cu layer (atoms 2 in **Figure 3**) do not contribute to the charge transfer. **Figure 5** shows the intensity measured through the Br K edge at (0 1 0.2), which probes the chemical character of the Br adatoms. A shift of the edge to lower energies at this position indicates that the Br 1s electrons are less tightly bound and implies that the Br adatoms carry a negative charge. The data shown in **Figures 4 and 5** are representative of a comprehensive data set and this is currently under analysis.

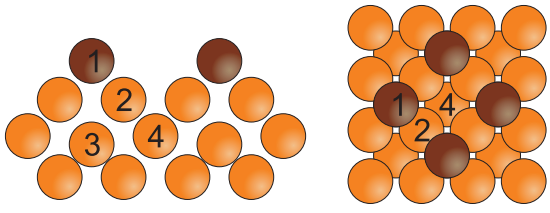

Figure 3: *Structural model of the c(2x2) adlayer on Cu(001).*

[1] H.C.N. Tolentino *et al.*, Surf. Sci. 601, 2962 (2007).
[2] Y. Gründer *et al.*, Phys. Rev. B 81, 174114 (2010).
[3] M. Saracino *et al.*, Phys. Rev. B 79, 115448-11 (2009).

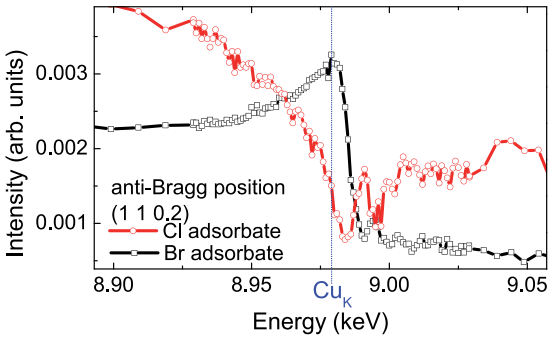

Figure 4: *Intensity at the anti-Bragg position of a Cu CTR (1 1 0.2) as the energy is scanned through the Cu K edge, for both Br and Cl adsorbates.*

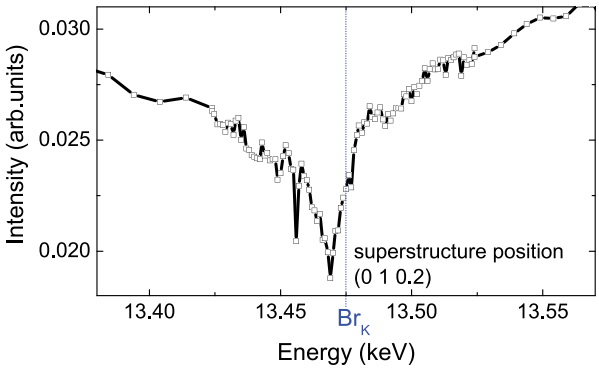

Figure 5: *Intensity at the superstructure position (0 1 0.2) as the energy is scanned through the Br K edge, for the Br-c(2x2) system.*

Double-q magnetic ordering in $GdNi_2B_2C$

M. Rotter, J. Jensen, C. Detlefs, J.A. Blanco and P.S. Normile – for further information contact M. Rotter, Max Planck Institute for Chemical Physics of Solids, Dresden, Germany.

martin.rotter@cpfs.mpg.de

Recently, experiments on certain 4f antiferromagnets with localized moments of high spin value but of zero orbital component have revealed a paradoxical situation with respect to expectations from theory. Namely, experiment has shown that symmetry-breaking lattice distortions in a zero applied magnetic field to be almost zero, a finding that contrasts with theoretical expectation and which has been coined the "magnetoelastic paradox" **[1]**. $GdNi_2B_2C$ (GNBC) is one such system. From scattering experiments on GNBC with neutrons **[1]** and x-rays **[2]**, using both resonant and non-resonant (x-ray) techniques, a *single-q* antiferromagnetic structure was determined. Such (single-q) ordering in GNBC is expected to be accompanied by a symmetry-breaking lattice distortion but none is found.

More recently a different type of magnetic ordering – a *double-q* structure – has been predicted for GNBC **[3]**. The results from the earlier scattering studies on GNBC do not contradict this new (calculated) structure. The magnetic Fourier components corresponding to the double-q structure comprise a first harmonic <q, 0, 0>, which may be associated with the magnetic satellites already observed in the previous scattering experiments **[1, 2]** and several types of higher harmonics: "mixed" harmonics, <2q, q, 0>, <q, 2q, 0> and a third harmonic <3q, 0, 0>. A special point about the predicted double-q structure is that it presents a way to resolve the magnetoelastic paradox in GNBC: interference between non-collinear Fourier components would reduce the orthorhombic distortion expected for the single-q scenario.

Theory predicts the scattering intensity at satellite positions corresponding to these higher harmonics to be considerably weaker than that at the first harmonic positions. Neglecting differences due to geometrical factors (e.g. the geometrical part of the relevant scattering cross-section, the Lorentz factor, the sample absorption factor), the scattering at the mixed harmonic satellite positions is expected to be around two orders of magnitude weaker than that at first harmonic positions, and at third harmonic positions even weaker scattering is expected. Here we report on a recent XMaS study, where resonant x-ray scattering has been employed to search for the higher harmonics associated with the double-q ordering in GNBC. Studying a single crystal sample of GNBC using x-rays tuned to the Gd L_2 edge, resonant satellite reflections consistent with such harmonics have been found below GNBC's Néel temperature ($T_N \approx 20$ K), and are shown in **Figure 6**. Panel (a) shows the resonant signal at a first harmonic satellite position, measured in the same study. At present we may conclude that our data are consistent with the prediction of double-q magnetic ordering in GNBC **[3].**

[1] M. Rotter *et al.*, Europhys. Lett. 75, 160 (2006).
[2] C. Detlefs *et al.*, Phys. Rev. B 53, 6355 (1996).
[3] J. Jensen and M. Rotter, Phys. Rev. B 77, 134408 (2008).

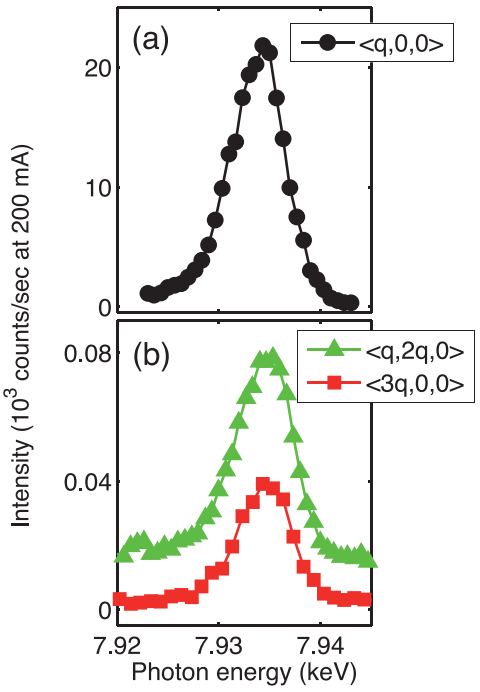

Figure 6: *Gd L_2 edge resonant signals measured at (a) the (q, 0, 4) and (b) the (q, 2q−1, 5) [green triangles] and the (3q−1, 0, 5) [red squares] satellite positions, where q ≈ 0.55 rlu (the legends give the corresponding Fourier components). The data, which are monitor corrected, were taken in the σ→π scattering channel at T = 2 K.*

Determining of the structure of tethered diblock copolymer films using a contrast enhancing agent

B. O'Driscoll, G. Newby, I. Hamley – for further information contact B. O'Driscoll, Department of Chemistry, University of Reading, Whiteknights, RG6 6AD, UK.

b.odriscoll@reading.ac.uk

Micro-phase separated tethered diblock copolymer films are of interest as they can form topographically smooth, but chemically patterned surfaces that are robust to abrasion. However only recently has their behaviour been examined in detail; the first theoretical model was published in 2010 **[1]**.

To validate this model we examined micro-phase separation in polystyrene-block-polymethyl methacrylate (PS-b-PMMA) films over a range of compositions (i.e. mole fraction of PS, xPS) **[2]**. As the electron density of the two blocks is almost identical it was necessary to use a contrast enhancing agent, ruthenium tetroxide - RuO_4 that reacts selectively with PS **[3]** leading to an increase in the electron density of the PS domains.

The principle focus of the experiments was to confirm the structure of the film normal to the surface. This was achieved using x-ray reflectometry (XRR) and fitting the electron density (ED) along Q_z (**Figure 7**). In line with the model, the electron density profiles showed that the PS domains are located at the air/film substrate, with the PMMA domains occupying the region closer to the substrate.

Using grazing incidence small angle x-ray scattering (GISAXS) it was also possible to measure the in-plane scattering of the samples. As expected the non-RuO_4 treated films showed no significant scattering, while the RuO_4 treated films produced at times very strong diffraction peaks (**Figure 8**), yielding periodicities of ~ 40 nm.

The use of the ruthenium stain did lead to an expansion of the PS domains. However, the pseudo 2D micro-phase separation in the films (with the polystyrene domains at the air/film interface) meant that this expansion could occur without changing the in-plane structure of the films. Moreover, by examining the relief patterns of the film using AFM it was possible to verify independently the phase assignments made for the films (**Figure 9**).

[1] M.W. Matsen, G.H. Griffiths, Eur. Phys. J. E, 29 (2), 219 (2009).
[2] B.M.D. O'Driscoll, G.E. Newby, I.W.Hamley, Polym. Chem., 2, 619-624 (2011).
[3] S.M. Park *et al.*, Macromol. Chem. Phys., 203 (14), 2069 (2002).

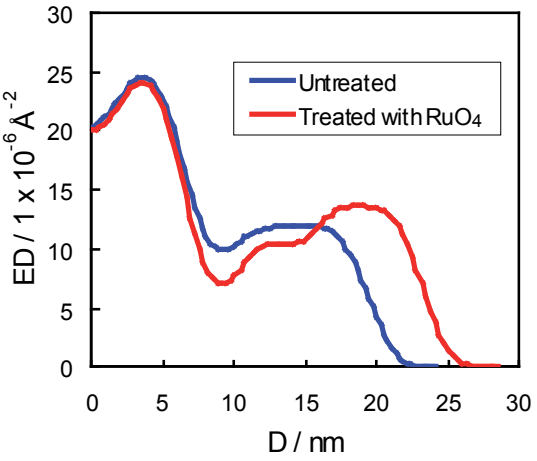

Figure 7: *Fitted electron density (ED) profiles extracted from the XRR data of a PS-b-PMMA film (xPS=0.26).*

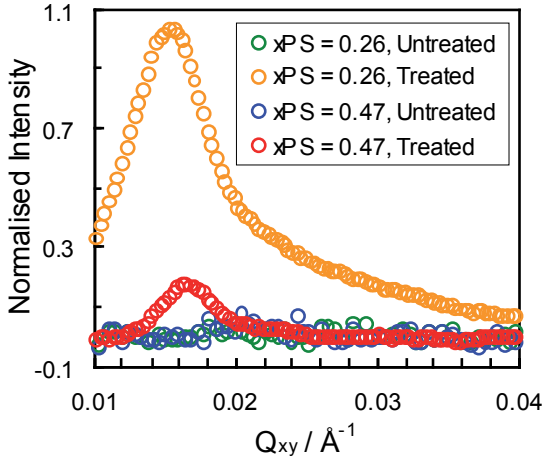

Figure 8: *In-plane profiles of various PS-b-PMMA films. The data were obtained using GISAXS before and after treatment.*

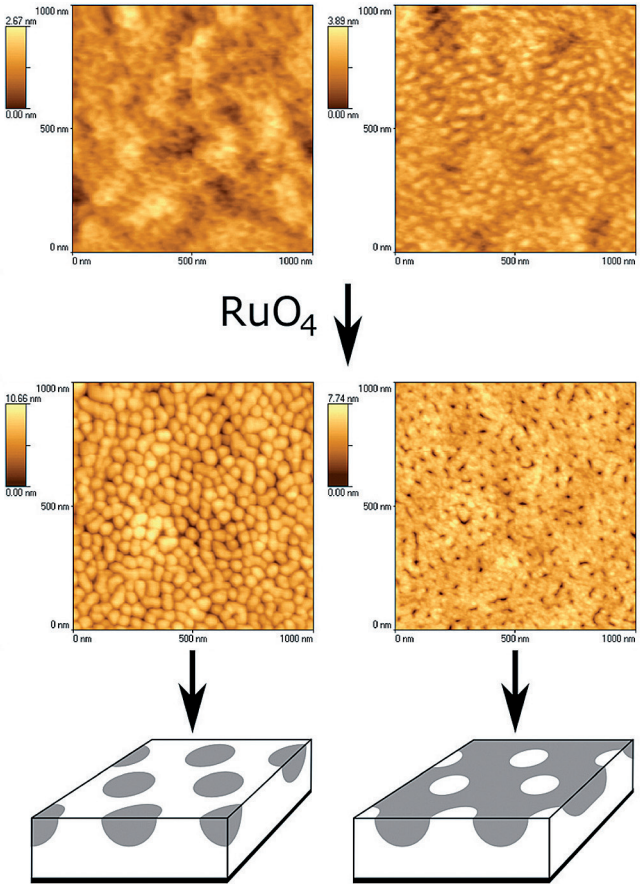

Figure 9: *AFM images of xPS = 0.26 (left) and xPS = 0.47 (right) PS-b-PMMA films prior to RuO_4 treatment (top), after treatment (middle) and schematics of the microphase separated films (bottom; the PS domains are coloured grey).*

Probing magnetic roughness in Fe/Pd/Au multilayers

J.A. González, T.P.A. Hase, L. Bouchenoire, P. S. Normile and B.J. Hickey – for further information contact J.A. González, Dto. Física Aplicada, Universidad de Castilla-La Mancha, 13071 Ciudad Real, Spain.

j.a.gonzalez@uclm.es

In artificially created structures composed of multiple layers the interface region often plays an important role in defining the properties of the final material. There have been many efforts to extract the chemical profile and interface roughness but relatively little effort has been devoted to the study of the magnetic profile and the truncation of any magnetic layers within the material **[1]**.

Fe/Au superlattices with submonolayer quantities of Pd deposited at each Fe/Au (and Au/Fe) interface have been prepared by Molecular Beam Epitaxy at the University of Leeds. By varying the amount of Pd at the interface we expect to control the amplitude of magnetic roughness. This expectation arises from the different magnetic anisotropies favoured at Fe-Pd and Fe-Au interfaces when the Fe layers are less than 5 monolayers (ML). For such thin layers, Fe moments in contact with Au tend to align perpendicular to the interface, while moments in contact with Pd prefer to point parallel to the interface (multilayer plane) **[2]**. Thus, in the case of partial Pd coverage, an enhanced magnetic roughness is expected in the Fe layer as depicted in the inset of **Figure 10**.

An Fe/Au multilayer with 0.75 ML (i.e. partial coverage) of Pd at each interface was studied using x-ray resonant magnetic reflectivity (XRMR). The sample contained 20 repeats of Fe(5 ML)/Au(16 ML) bilayers. The 3.173 keV (Pd L_3 edge) incident photons were circularly polarised by means of a 0.1 mm diamond phase-plate. The magnetic reflectivity is defined in terms of the *flipping ratio,* $(I^+–I^-)/(I^++I^-)$. This was measured as a function of momentum transfer perpendicular to the multilayer plane (Q_z) and applied magnetic field. The quantities I^+ and I^- denote the specular intensity measured when the sample magnetization and incident beam helicity vectors are parallel and antiparallel, respectively.

Consistent flipping ratios were found using two different methods employing the same *magnitude* of magnetic field applied to the sample: *method i)* working with fixed incident helicity while reversing the direction of the applied field and *method ii)* keeping the direction of the field fixed while reversing the sense of the helicity.

Figure 10b shows the magnetic reflectivity (obtained by *method i)* as a function of momentum transfer. Also shown in the figure is a qualitative simulation of this magnetic reflectivity (panel c) and the standard specular reflectivity (panel a). The simulation shown in panel c was obtained from the difference of two calculated reflectivities corresponding to the same structure but with slightly different Pd layer densities (differing by 4 %). This change in density produces a small change in the refractive index and models the similar effect associated with the change in sign of the magnetic scattering amplitude between the parallel (+) and antiparallel (–) vector settings. We note that this is not a quantitative model, but it reproduces the main features seen in panel (b). The strong effect seen at the position of the 4th Bragg peak is due to the ratio of the Fe to Au layer thicknesses.

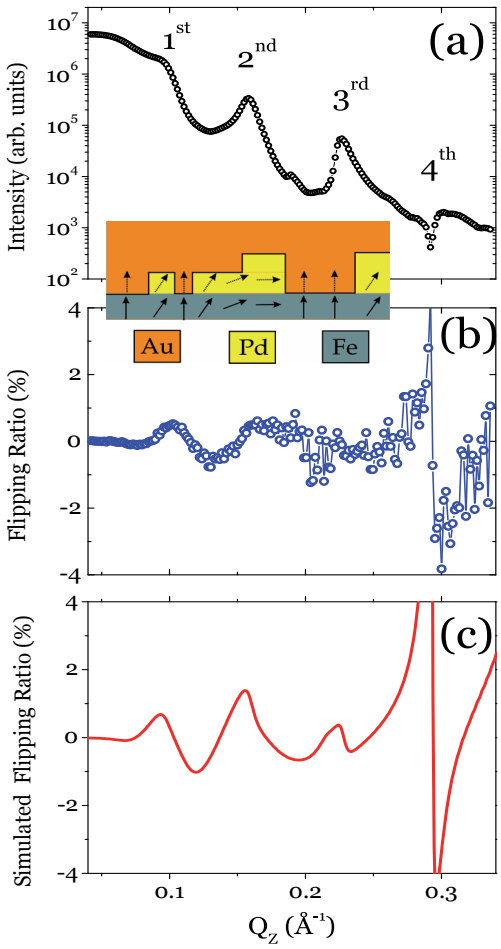

Figure 10: *Measured (b) and simulated (c) magnetic reflectivity. Shown for comparison in (a) is the standard reflectivity (= sum of I^+ and I^-), where the n^{th} Bragg peaks are labelled. The inset shows a schematic of the hypothetical moment directions at a given interface in the multilayer.*

Figure 11 shows the magnetic field dependence of the flipping ratio at the first Bragg peak (obtained by *method ii)* compared to the hysteresis loop obtained via bulk vibrating sample magnetometry (VSM). The main panel shows the two positive field branches of the dependence, while the inset shows the complete loop. Since the field is applied in the multilayer plane, which is the anisotropy favoured by Fe-Pd, one might expect that the Fe-Pd regions saturate prior to the Fe-Au regions and that magnetic disorder (roughness) exists at intermediate field values. This behaviour would be experimentally supported if one observed the flipping ratio to saturate more rapidly than the VSM signal. The flipping ratio is element specific and only probes the Pd and hence the Fe-Pd moment. On the other hand, the VSM signal represents the total averaged Fe moment direction with respect to the applied field.

The flipping ratio data in **Figure 11**, although noisy, possibly suggest such a difference. By measuring at low temperature in future studies (to increase the magnetic susceptibility of Pd) we hope to confirm or otherwise this behaviour.

[1] S. Langridge *et al.*, Phys. Rev. B 74 014417 (2006).
[2] F. Zavaliche *et al.*, J. Phys. D Appl. Physics 36, 779 (2003).

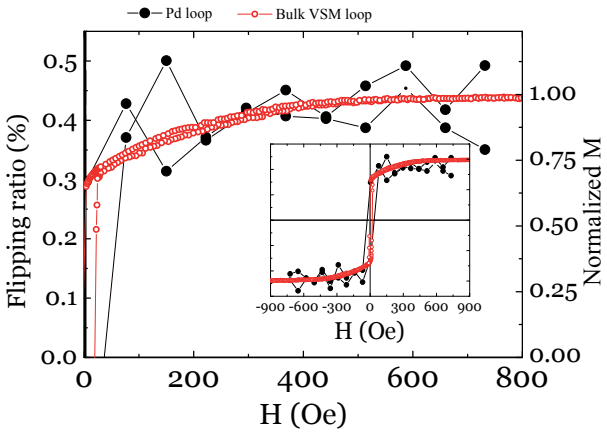

Figure 11: *Hysteresis loops measured by bulk magnetometry (open circles in red) and at Q_z=0.0965 Å^{-1} being the position of the first superlattice Bragg peak (black dots) during a standard field cycle (hysteresis loop) at the Pd L_3 edge.*

In-situ electric polarisation measurements of multiferroic $TmMn_2O_5$

R.D. Johnson, P. Thompson, S.R. Bland, L. Bouchenoire, H. Kimura, Y. Noda and P.D. Hatton – for more information contact R.D. Johnson, Department of Physics, University of Oxford, Parks Road, Oxford, OX1 3PU, UK.

r.johnson1@physics.ox.ac.uk

Multiferroic materials have the potential for becoming key components in novel data storage and sensor solutions, and so are of great interest to condensed matter researchers. Some of the most extreme mutliferroic phenomena have been observed in the RMn_2O_5 series (R = rare earth, Bi or Y), in which a ferroelectric polarisation is induced by magnetism in a single phase. For example, magnetically induced electric polarisation flips and flops have been reported in $TbMn_2O_5$ **[1]** and $TmMn_2O_5$ **[2]**, respectively. However, these technologically exciting phenomena originate in an elusive magneto-electric coupling mechanism that remains the subject of debate. The most probable origin of multiferroicity in this series is the exchange-striction mechanism **[3]**, whereby the magnetism is predicted to couple to the crystal lattice through magnetostriction, giving rise to small structural modulations that break inversion symmetry and hence induce a net electric polarisation. In this experiment we directly test the exchange-striction model in $TmMn_2O_5$ by performing an *in-situ* measurement of the electric polarisation, simultaneously with a measurement of x-ray diffraction signals that originate in the structural modulation. Such measurements, pioneered at XMaS, have only recently been made possible.

A high quality, single crystal sample of $TmMn_2O_5$ was prepared with gold contacts evaporated onto two surfaces cut with the *b*-axis surface normal. A third surface was cut and polished to a mirror like finish for diffraction, with the *c*-axis surface normal. The electric polarisation was measured through the main ferroelectric phase by applying a 20 Hz sinusoidal high voltage and integrating the current. The resultant $D(t)$ vs. $E(t)$ loops are shown in **Figure 12** from which the remnant polarisation was directly inferred.

Figure 13 shows the temperature dependence of the remnant polarisation, and also that of the magneto-striction diffraction signal, through the main ferroelectric phase. This figure shows the evolution of the electric polarisation 2 K above the upper phase boundary at T_D, as previously reported in the literature **[4]**. The magneto-striction then develops with the same temperature dependence as the polarisation, indicating a strong coupling. Below 30 K we have observed an interesting result: the electric polarisation vanishes, whilst the magneto-striction remains prominent down to the lower phase boundary. This poses new questions with regard to the magneto-electric coupling, and will form the basis of future diffraction studies.

[1] N. Hur *et al.*, Nature 429, 392 (2004).
[2] M. Fukunaga *et al.*, Phys. Rev. Lett. 103, 077204 (2009).
[3] P.G. Radaelli *et al.*, Phys. Rev. Lett. 101, 067205 (2008).
[4] M. Fukunaga *et al.*, J. Phys. Soc. Jpn. 77, 094711 (2008).

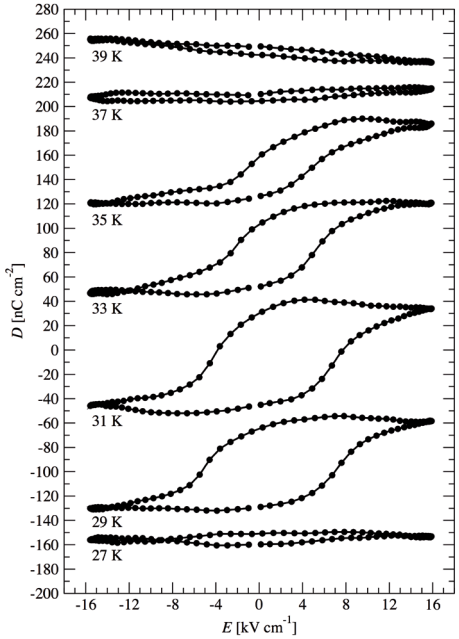

Figure 12: *D(t) vs. E(t) loops measured through the main ferroelectric phase of $TmMn_2O_5$. The curves have been offset for clarity.*

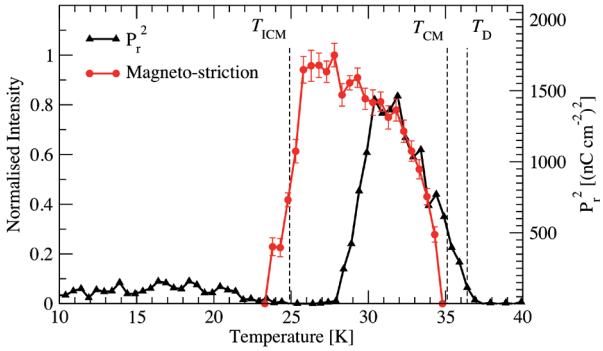

Figure 13: *Temperature dependence of the magneto-striction diffraction signal (red) and the remnant electric polarisation (black) measured at XMaS.*

In-situ grazing incidence diffraction during processing of organic solar cells

S. Lilliu, T. Agostinelli, M. Hampton, E. Pires, J. Nelson and J.E. Macdonald – for further information contact J. Emyr Macdonald, School of Physics and Astronomy, University of Cardiff, CF24 3AA UK.

macdonald@cardiff.ac.uk

In organic photovoltaics, the exciton diffusion length is of the order of 10-20 nm **[1]**. Charge separation occurs at donor-acceptor interfaces and hence efficient conversion of absorbed photons requires that excitons are generated very close to such an interface. This is achieved in bulk-heterojunction (BHJ) solar cells **[1-5]** using a nanoscale blend of donor and acceptor materials (such as a conjugated polymer and a fullerene). In addition to this requirement for sufficiently intimate mixing of the donor and acceptor phases for charge separation, efficient transport of separated charges towards the electrodes requires a certain degree of phase segregation between the two materials, to enable ordered molecular packing within each phase and also minimize interfacial recombination. The optimum microstructure is thus a compromise between intimate mixing and complete segregation of the two phases **[6]**.

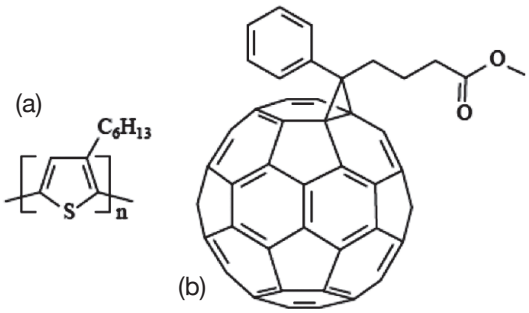

Figure 14: *Molecular structure of (a) P3HT (b) PCBM.*

The blend of poly(3-hexylthiophene) (P3HT) with [6,6]-phenyl-C61-butyric acid methyl ester (PCBM) is the best studied materials system (**Figure 14**) for organic photovoltaic applications with a power conversion efficiency close to 5% **[1]**. High photocurrents are obtained after a thermal annealing process which leads to crystallization of the polymer and formation of aggregates of PCBM. This high degree of phase segregation seems to be driven by the strong tendency of the polymer chains to crystallize, expelling PCBM from the polymer

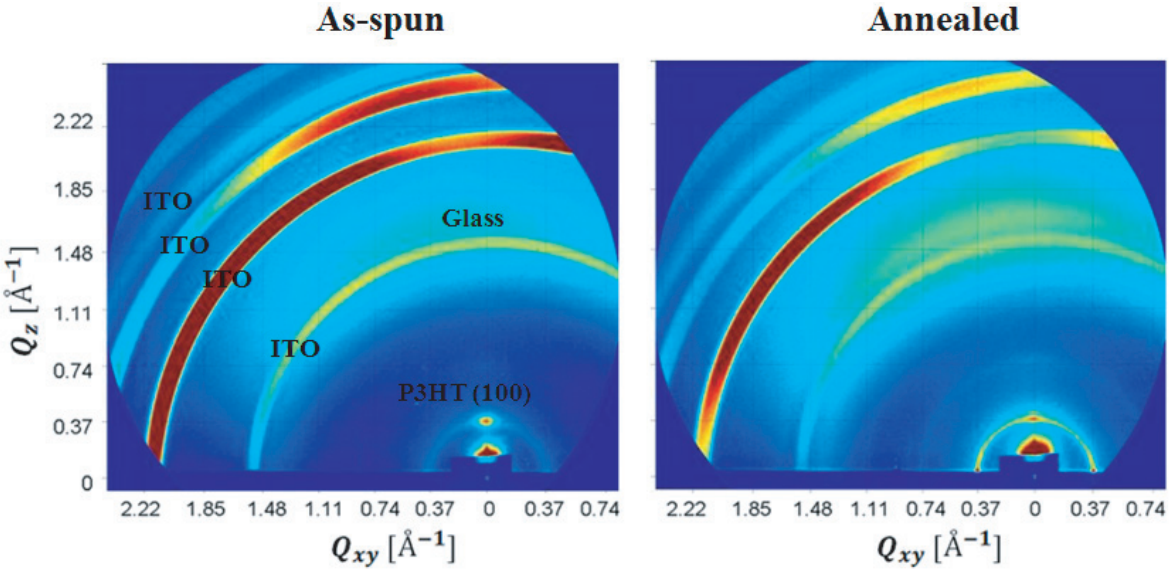

Figures 15: *GIXRD images for an as-spun and annealed glass/ITO/PEDOT-P3HT/PCBM/Al sample.*

domains. Device structures comprise a ~100 nm film of the P3HT:PCBM blend deposited onto transparent indium tin oxide (ITO) treated with PEDOT:PSS with an aluminium top electrode, the structure being typically annealed at 140°C.

In a collaboration between the groups at Cardiff and Imperial College, we have performed time-resolved grazing incidence x-ray diffraction (GIXRD) during *in-situ* annealing of the full device structures **[7]** (**Figure 15**). Images were acquired with a time increment of 18 s before, during and after the in-situ anneal. Processing conditions were simulated by rapid heating to 140°C.

Out-of-plane (OOP) radial sections were extracted, and domain sizes were calculated from the P3HT (100) peak widths ΔQ, using the Debye-Scherrer formula $L_{100} \approx 0.9 \times 2\pi/\Delta Q$. This is an approximation which ignores paracrystalline disorder, whose effect on the low-Q (100) peak is relatively weak. In **Figure 16**, the resulting domain size is shown alongside the temperature profile during the anneal. It is clear that the dramatic changes in P3HT domain size occur in the first minutes of the anneal.

This rapid crystallisation is consistent with our studies of the power conversion efficiency (PCE) of P3HT:PCBM devices annealed for different times. **Figure 17** shows that the first few minutes of the anneal are crucial to improve the efficiency. Analysis of other structural effects are in progress. A detailed understanding of the structural changes occurring during *in-situ* processing is fundamental to the development of new organic photovoltaic polymers.

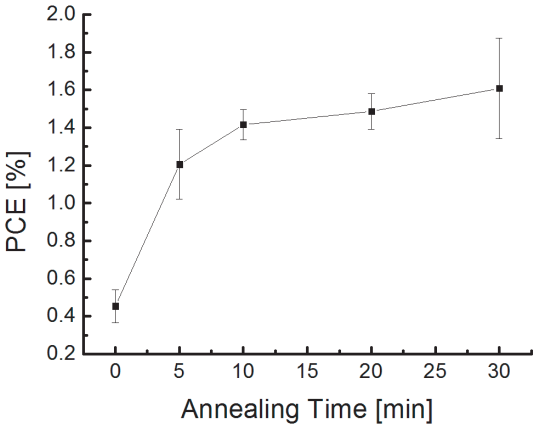

Figure 17: *Power Conversion Efficiency (PCE) as a function of annealing time. The efficiency increases rapidly during the first five minutes, coinciding with the rapid increase in domain size* ***(Figure 16)****.*

[1] D. Carsten, D. Vladimir, Rep. Prog. Phys. 73, 096401 (2010).
[2] N.S. Sariciftci *et al.*, Science 258, 1474 (1992).
[3] B.C. Thompson, J.M.J. Fréchet, Polymer-Fullerene Composite Solar Cells, Angew. Chem., Int. Ed. 47, 58 (2008).
[4] T.N. Ng *et al.*, Appl. Phys. Lett. 92, 213303 (2008).
[5] S.F. Tedde *et al.*, Nano Lett. 9, 980 (2009).
[6] E. Verploegen *et al.*, Adv. Funct. Mat. 20, 3519 (2010).
[7] T. Agostinelli *et al.*, Adv. Funct. Mat., DOI: 10.1002/adfm.201002076 (2011).

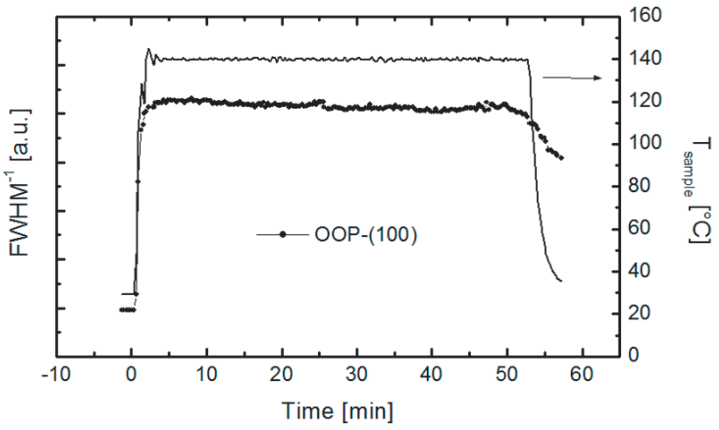

Figures 16: *Evolution of the Debye Scherrer domain size during annealing for P3HT approximated from the out-of-plane-(100) peak FWHM (dotted line). The temperature of the sample during annealing is also shown (black line).*

Interplay of inequivalent atomic positions in resonant x-ray diffraction of Fe_3BO_6

G. Beutier, E. Ovchinnikova, S.P. Collins, V.E. Dmitrienko, J.E. Lorenzo, J.-L. Hodeau, A. Kirfel, Y. Joly, A.A. Antonenko, V.A. Sarkisyan and A. Bombardi – for further information contact G. Beutier, SIMaP, Grenoble, France.

guillaume.beutier@simap.grenoble-inp.fr

Screw-axis and glide-plane "forbidden" Bragg reflections are sometimes observed in resonant x-ray scattering (RXS) experiments due to the anisotropy of the scattering tensor **[1]**. They yield information on the electronic environment of the resonant atoms, sometimes related to charge, orbital or magnetic order. An interesting aspect of the technique is its chemical selectivity, since it probes only the resonant species. However, the contributions of ions of the same species occupying inequivalent crystallographic sites are difficult to disentangle unless additional reflection conditions apply to one of the sites. It can nevertheless be achieved by measuring several forbidden reflections, as demonstrated here in the case of iron orthoborate (Fe_3BO_6). In Fe_3BO_6 (space group *Pnma*), Fe ions occupy two inequivalent atomic positions: a general position (8d) in distorted oxygen octahedra and a special position (4c) in oxygen tetrahedra **[2]**. The special position 4c does not have additional reflection conditions.

We measured several (h00) reflections with h-odd, which are forbidden by a glide-plane, in the vicinity of the Fe K edge (~7.12 keV) **[3]**. These resonant reflections produce several tens of thousands counts per second. Different electronic multipole transitions compete in the scattering amplitudes of the two sites: dipole-dipole (E1-E1), dipole-quadrupole (E1-E2) and quadrupole-quadrupole (E2-E2). The E2 contribution was evidenced in the pre-edge region of the forbidden reflection spectra, in particular by its azimuthal dependence with up to 6-fold harmonic components (**Figure 18**). Non-resonant magnetic scattering was also evidenced below the edge, due to the magnetic order. All three resonant processes fully rotate the x-ray linear polarization from perpendicular (σ) to parallel (π) to the scattering plane, so that the measurements could be done with the natural horizontal polarization delivered by the beamline and without any secondary polarization analyser.

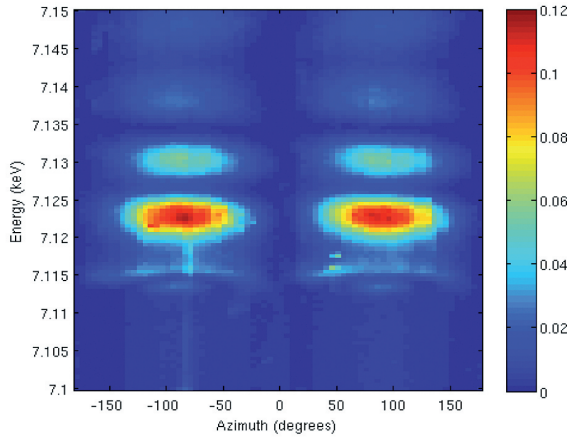

Figure 18: *Energy-Azimuth map of the (700) forbidden reflection (intensities on a linear scale of colour, in arbitrary units). The E2 features can be seen around 7.113 keV and in* ***Figure 19****.*

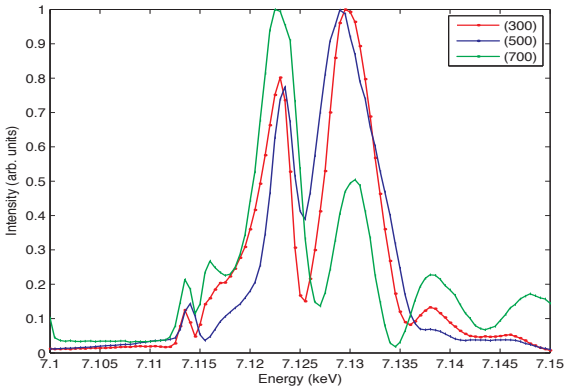

Figure 19: *Normalized intensity spectra of the (300), (500) and (700) reflections measured at the same azimuthal angle of 90°. The (500) is actually ~3 times stronger than the (300) and ~9 times stronger than the (700).*

We measured the (300), (500) and (700) forbidden reflections (**Figure 19**), in which the structure factor F_{8d}(h00) and F_{4c}(h00) vary differently. At the (300) reflection, the structure factor of the 4c sites nearly vanishes, and the signal is largely dominated by the 8d sites; at the (500) reflection, the amplitudes from both sites add constructively, yielding a large intensity, while at the (700) reflection they add destructively, yielding a weak intensity and strong interferences in the spectrum.

With the help of the FDMNES code **[4]**, we were able to reproduce the spectra of the three measured reflections (not shown here) by optimizing the two site contributions. We found evidence of a chemical shift of 0.7 eV, related to the different environments of the ions, between the two fundamental spectra **[3]**.

[1] V.E. Dmitrienko, Acta Cryst. A 39, 29 (1983).
[2] J.G. White *et al.*, Acta Cryst .19, 1060 (1965).
[3] G. Beutier *et al.*, J. Phys.: Condens. Matter 21, 265402 (2009).
[4] www.neel.cnrs.fr/fdmnes

In-situ real time structural response of ferroelectrics to an external electric field

S.H.M. Ryding, T.L. Burnett, S.D. Brown, M. Cain, R.J. Cernik, M. Stewart, P. Thompson – for further information contact S.H.M. Ryding, University of Manchester, Materials Science Centre, Manchester M17HS,UK.

stephanie.ryding@postgrad.manchester.ac.uk

Ferroelectrics exhibit spontaneous polarisation below their Curie temperature and contain areas of uniform polarisation known as domains which can be switched by the application of an electric field. These materials have many applications for actuators, sensors and switches. Relaxor ferroelectrics exhibit frequency dependent behaviour. What is not well understood is how this switching behaviour is related to frequency. There are very few X-ray scattering stations anywhere in the world that provide the ability to switch an external electric field whilst simultaneously observing the changes in crystal structure.

In a recent experiment carried out at XMaS, a single crystal of $Pb[Mn_{1/3}Nb_{1/3}]O_3$-0.32$PbTiO_3$ (PMN-0.32PT) was mounted on a sapphire support. The electrical contacts were made on the (110) faces. The crystal was poled along the <100> direction. The electrical response and the diffraction data were measured simultaneously under the application of either a constant or oscillating electric field. The static measurements were used to verify the range of the reciprocal space map to study whereas the dynamic measurements aimed to study the sample structure changes.

Figure 20 shows the existence of a shift of the (200) Bragg peak under the application of a constant field of 4kV/mm.The diffraction data were then collected for different applied voltages (from 0-4kV in 0.2kV intervals) at 0.01Hz, 0.1Hz and 1Hz. The single crystal was found to contain two crystallographic phases, tetragonal (*P4mm*) and monoclinic (*Cm*). **Figure 21** shows the crystal's response to the applied electric field in terms of the transformation from the monoclinic phase to the tetragonal phase. The percentage of each phase was obtained by a nonlinear least squares method based on fitting the (200), (220) and (222) peak profiles. It can be seen that the phase transition is dependent on the electric field frequency with the observed structural changes being less marked at higher frequencies.

We plan to extend these studies further to obtain a more detailed understanding of the mechanisms involved in relaxor switching. The electric field waveform and voltage generator system is being replicated at the DIAMOND light source on beamline I11 to study polycrystalline materials, thin films and multilayers. This will provide complementary facilities to XMaS where single crystal ferroelectric studies will be continued. The ultimate aim of these experiments is to follow crystallographic structure changes as a function of applied field and to correlate these changes with macroscopic physical properties.

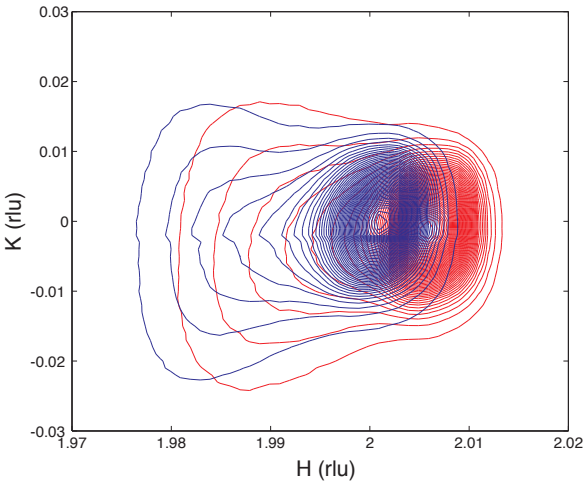

Figure 20: *(200) peak without (blue) and with (red) an external voltage of 4kV/mm. A shift of the Bragg peak position by approximately 0.005 r.l.u. in the H direction is observed when the electric field is applied.*

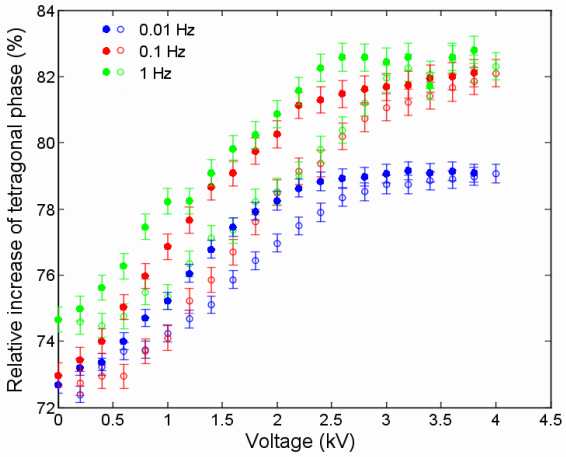

Figure 21: *Percentage change of the tetragonal phase relative to the coexisting monoclinic phase. This change was observed as a function of applied voltage and for three different frequencies: 0.01Hz (blue), 0.1Hz (red) and 1Hz (green). An hysteretic response is observed when the voltage is ramped up (open circles) and then ramped down(filled dots). The data show that the structural changes are less marked as the frequency increases. In fact the response at 0.1 and 1 Hz is very similar.*

➡ Please note

Some of the experimental reports in the previous pages are as yet unpublished. Please email the contact person if you are interested in any of them or wish to quote these results elsewhere.

➡ Our web site

www.esrf.eu/UsersAndScience/Experiments/CRG/BM28/
It contains the definitive information about the beamline and the on-line beamline manual.

➡ Living allowances

These are still 55 euros per day per beamline user – the equivalent actually reimbursed in pounds sterling, of course. XMaS will support up to 3 users per experiment. This is not a restriction on the number of experimentalists but you should make your own budgetary arrangements for those in excess of 3. The ESRF hostel still appears adequate to accommodate all our users, though CRG users will always have a lower priority than the ESRF's own users. Do remember to complete the web-based "A form" requested of you when you receive the ESRF invitation, all attendees must be listed, since this informs the safety group of the attendees and is used to organise all site passes, meal cards and accommodation.

➡ Beamline people

The personnel changes which occurred during the last fifteen months were described in the Introduction to this Newsletter.
Beamline Responsible – Simon Brown (sbrown@esrf.fr).
Beamline Coordinator – Laurence Bouchenoire, (boucheno@esrf.fr), is the person who can provide you with general information about the beamline, application procedures, scheduling, etc. Laurence should normally be your first point of contact.
Beamline Scientists – Simon Brown (sbrown@esrf.fr), Oier Bikondoa (oier.bikondoa@esrf.fr) and Didier Wermeille (didier.wermeille@esrf.fr).
Post-Doc – Gemma Newby (gemma.newby@esrf.fr).
Technical Support – Paul Thompson (pthompso@esrf.fr) continues to work on instrument development and provides technical support for the beamline. John Kervin (jkervin@liv.ac.uk), who is based at Liverpool University, provides further technical back-up and spends part of his time on-site at XMaS.
Project Directors – Malcolm Cooper (m.j.cooper@warwick.ac.uk), Chris Lucas (clucas@liv.ac.uk) and more recently Tom Hase (T.P.A.Hase@warwick.ac.uk) continue to travel between the UK and France to oversee the operation of the beamline. The administration for XMaS continues to be handled by Sandra Beaufoy at Warwick University (s.beaufoy@warwick.ac.uk).

➡ The Project Management Committee

The current membership of the committee is as follows:
- Bob Cernik (chair)
- Denis Greig
- Peter Hatton
- Chris Nicklin
- David Bradley
- Andrew Boothroyd
- Colin Norris
- Jonathan Williams

meeting twice a year, in addition to the above, the directors, the chair of the Peer Review Panel and the beamline team are in attendance.

➡ The Peer Review Panel

The current membership of the panel is as follows:
- Sean Langridge (chair)
- Paul Strange
- Carsten Detlefs
- Steve Collins
- Geetha Balakrishnan
- Karen Edler

In addition either Malcolm Cooper, Tom Hase or Chris Lucas attends their meetings.

➡ Housekeeping!!

At the end of your experiment samples should be removed, tools, etc returned to racks and unwanted materials disposed of appropriately. When travel arrangements are made, therefore, please allow additional time to effect a tidy-up.

➡ PUBLISH PLEASE!!… and keep us informed

Although the list of XMaS papers is growing we still need more of those publications to appear. We ask you to provide Sandra Beaufoy not only with the reference but also a preprint/reprint for our growing collection. Note that the abstract of a publication can also serve as the experimental report!

➡ IMPORTANT!

When beamline staff have made a significant contribution to your scientific investigation you may naturally want to include them as authors. Otherwise we ask that you add an acknowledgement, of the form: "This work was performed on the EPSRC-funded XMaS beamline at the ESRF, directed by M.J. Cooper, C.A. Lucas and T.P.A Hase. We are grateful to S.D. Brown, O. Bikondoa, D. Wermeille, G. Newby, L. Bouchenoire and P. Thompson for their invaluable assistance, and to S. Beaufoy and J. Kervin for additional support."

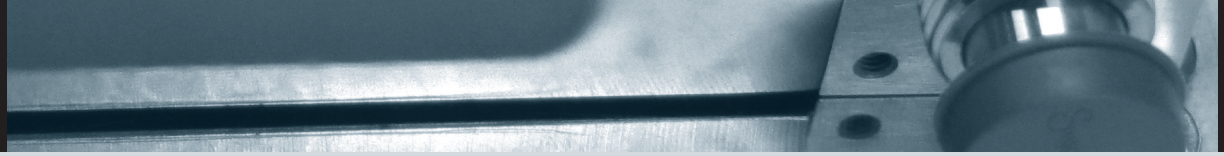

Guidelines

for beam-time applications

➠ Beamline Operation

The XMaS beamline at the ESRF, which came into operation in April 1998, has some 133 days of beam time available each year for UK user experiments, after deducting time allocated for ESRF users, machine dedicated runs and maintenance days. During the year, two long shut-downs of the ESRF are planned: 4 weeks in winter and 4 weeks in summer. At the ESRF, beam is available for user experiments 24 hours a day.

➠ Applications for Beam Time

Two proposal review rounds are held each year, with deadlines for submission of applications, normally, the end of March and September for the scheduling periods August to end of February, and March to July, respectively. Applications for Beam Time are to be submitted electronically (the paper versions are not acceptable) following the successful model used by the ESRF and ourselves. Please consult the instructions given in the ESRF web page:

www.esrf.eu

Follow the links: **"User Portal"** under **"Quick Links"**
Enter your surname and password
and select: **"Proposals/Experiments"**

Follow the instructions carefully – you must choose "CRG Proposal" and "XMAS-BM28" at the appropriate stage in the process. A detailed description of the process is always included in the reminder that is emailed to our users shortly before the deadline – for any problems contact L. Bouchenoire, as above.

Technical specifications of the beamline and instrumentation available are described in the XMaS web page.
When preparing your application, please consider the following:

■ All sections of the form must be filled in. Particular attention should be given to the safety aspects, and the name and characteristics of the substance completed carefully. Experimental conditions requiring special safety precautions such as the use of lasers, high pressure cells, dangerous substances, toxic substances and radioactive materials, must be clearly stated in the proposal. Moreover, any ancillary equipment supplied by the user must conform with the appropriate French regulations. Further information may be obtained from the ESRF Experimental Safety Officer, tel: +33 (0)4 76 88 23 69; fax: +33 (0)4 76 88 24 18.

■ Please indicate your date preferences, including any dates that you would be unable to attend if invited for an experiment. This will help us to produce a schedule that is satisfactory for all.

■ An experimental report on previous measurements must be submitted. New applications will not be considered unless a report on previous work is submitted. These also should be submitted electronically, following the ESRF model. The procedure for the submission follows that for the submission of proposals – again, follow the instructions in the ESRF's web pages carefully. **Reports must be submitted within 6 months of the experiment**.

■ The XMaS beamline is available for one third of its operational time to the ESRF's user community. Applications for beamtime within that quota should be made in the ESRF's proposal round - **Note: their deadlines are earlier than for XMaS! - 1st March and 1st September.** Applications for the same experiment may be made both to XMaS directly and to the ESRF. Obviously, proposals successfully awarded beamtime by the ESRF will not then be given beamtime additionally in the XMaS allocation.

➠ Assessment of Applications

The Peer Review Panel for the UK-CRG considers the proposals, grades them according to scientific excellence, adjusts the requested beam time if required, and recommends proposals to be allocated beam time on the beamline.
Proposals which are allocated beam time must in addition meet ESRF safety and XMaS technical feasibility requirements.
Following each meeting of the Peer Review Panel, proposers will be informed of the decisions taken and some feedback provided.

XMaS the UK-CRG
is an EPSRC sponsored project

XMaS, ESRF, 6 rue Jules Horowitz BP 220, 38043 Grenoble Cedex 9, France
Tel: +33 (0)4 76 88 25 80; Fax: +33 (0)4 76 88 24 55
web page : www.esrf.eu/UsersAndScience/Experiments/CRG/BM28/ – email: boucheno@esrf.f

Editor: L. Bouchenoire – Layout: ICCS/J.-C. Irma – Print: Warwickprinting – March 2011

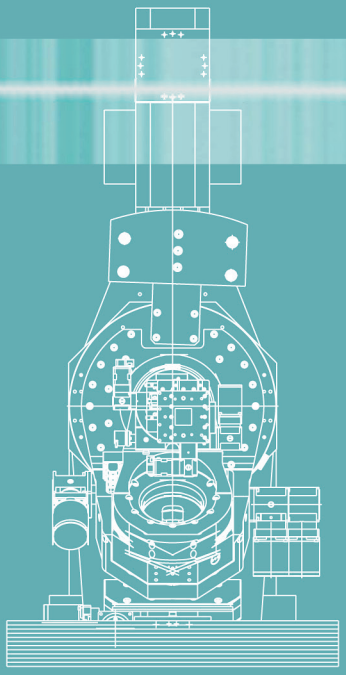

New: Modular Beam Conditioning Unit

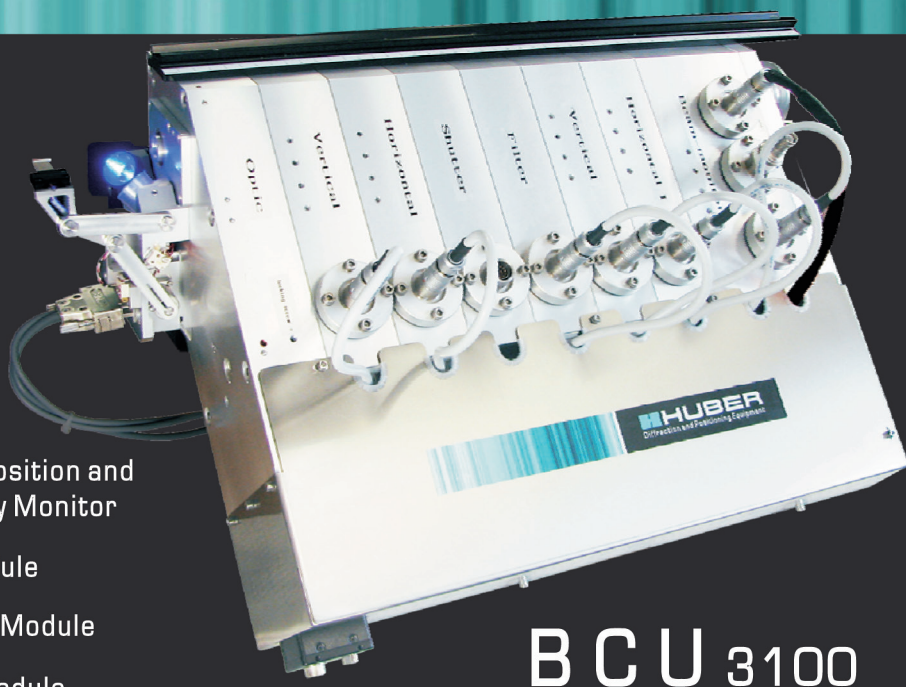

- Beam Position and Intensity Monitor
- Slit Module
- Shutter Module
- Filter Module
- Protein Crystallography Unit

BCU 3100

We make the Best of your Beam

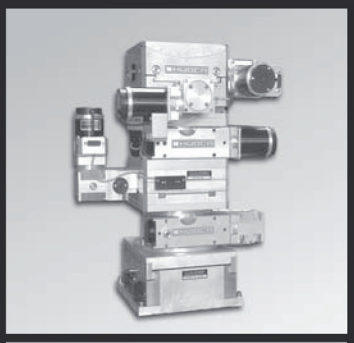

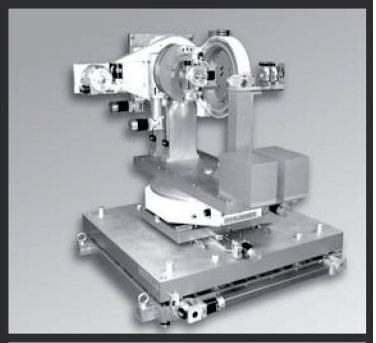
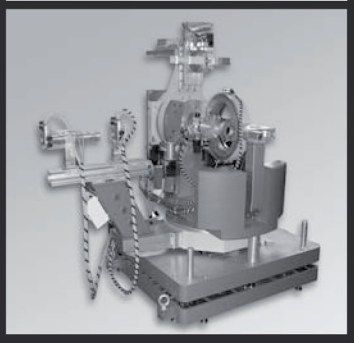
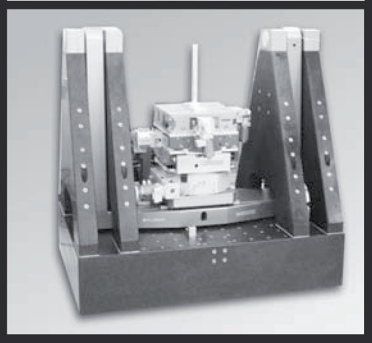


X-Ray Diffractometers and Cameras

Multiaxis Goniometers
for X-Ray-, Synchrotron- and Neutron Facilities

Monochromators

Positioning Devices
for Various Environments

Custom Built Instruments

Electronics

Accessories

HUBER Diffraktionstechnik GmbH & Co. KG
Sommerstrasse 4
D-83253 Rimsting, Germany

www.xhuber.com
info@xhuber.com

HUBER
Diffraction and Positioning Equipment